

# Feasibility study of low power helicon thruster

M. Manente<sup>a</sup>, M. Walker<sup>b</sup>, J. Carlsson<sup>c</sup>, C. Bramanti<sup>d</sup>, S. Rocca<sup>e</sup>, D. Curreli<sup>a</sup>, Y. Guçlu<sup>a</sup>, D. Pavarin<sup>a</sup>

- a) *CISAS University of Padua Via Venezia 15 35131 Padova Italy*
- b) *Georgia Tech University Atlanta, GA*
- c) *Txcorp Boulder Colorado USA*
- d) *Advanced Concept Team ESA ESTEC*
- e) *ONERA (Paris)*

## Abstract

Helicon thrusters have been recently considered a possible new electric propulsion system thanks to the acceleration mechanism called “current free double layer “ which allows specific impulse up to 1300 s applying Argon and 4000 s applying hydrogen.

Although the primary interest of this technology was always regarding primary propulsion, on this paper is explored the possibility of using helicon thruster for secondary propulsion e.g. station keeping or attitude control onboard of satellite from mini to telecommunication class.

Such a thruster provides several advantage respect to the electric propulsion system currently applied: (i) is build up by very few components, thus is reliable, (ii) thrust and power can be modulated, thus it is versatile, (iii) plasma interact marginally with the thruster structure, thus erosion is not an issue, (IV) is light and compact.

The numerical analysis have been conducted through a combination of 1-D and 2-D numerical code. A specific 1-D code named PPDL has been developed to simulate potential drop acceleration. Main feature of the code are: hybrid Boltzmann electron/drift-kinetic ion, inclusion of dominant 2D effects, high computational efficiency thorough implicit non linear Boltzmann solver. The 2D code XOOPIC is free available from Berkeley University. Limitations of XOOPIC are no floating boundary condition implemented on the electrostatic solver and long computational time. The combined approach resulted very useful since the 1-D code has been used to screen many different experimental conditions and to identify the right boundary condition. 2-D code has been then used to refine 1-D results. The two models, combined with a global model specifically developed to simulate the plasma reaction inside the plasma source, have been finally run, through genetic algorithms to identify an optimal thrusters configuration in the 50 W power regimes.

## 1. Introduction

Recently a strong interest in micro-propulsion has arisen within the space community: These devices will required to deliver very low thrust values (millinewtons and below) and low impulse bits and should be characterize by engine masses and sizes smaller than current propulsion technology. Interest in such devices is driven by the needs of the most advanced missions currently being studied within the scientific space communities. Because a large fraction of launch costs consists of safety procedures surrounding the storage, handling, and loading of toxic and/or carcinogenic propellants used by established propulsion systems, additional cost savings can be

obtained by utilizing environmentally safe propellants, with better performance and/or storage characteristics than existing monopropellants.

These needs involve primary propulsion and attitude control of micro-spacecraft having total wet mass around few kilograms and precise positioning control of spacecraft constellation. Micropropulsion systems require miniature feed system components, such as valves, pressure regulators, flow controllers, tanks. Thus, development of new propulsion hardware requires advanced microfabrication techniques, such as MEMS technology. Spacecraft with mass less than 100 kg, but larger than a few tens of kilograms, may still be characterized by subsystem architectures that follow traditional design approaches to a large extent, in both component design and integration. To enable an order of magnitude reduction in spacecraft size while retaining mission capabilities, further developments in propulsion technology are needed.

Three classes of electric propulsion devices are currently in use or near being used in flight. These types are referred to as electrothermal, electrostatic, or electromagnetic devices, depending on the principle by which the working fluid is accelerated to provide thrust. Electrothermal thrusters create a high temperature fluid which provides a driving force by acceleration through a conventional nozzle. The thermal energy of the fluid is partly converted to kinetic energy. Electrostatic thrusters provide thrust by accelerating a charged plasma by means of a static electric field. Electromagnetic thrusters apply an electromagnetic field to accelerate an electrically charged plasma. This electromagnetic field can be self-induced or externally generated. The least complex electric propulsion system available is the resistojet. In a hydrazine resistojet, the heat of the products of hydrazine, decomposed in a catalyst bed, is resistively augmented in a heating coil. The increase in performance over monopropellants can range to 80 s, but this requires 0.3-0.4 kW of electric power.

### Hydrazine monopropellant thruster

Hydrazine monopropellant thruster combine engine technology substantially simple than that of bipropellant engines with a high reliability, relatively simple feed system and intermediate performance characteristics (specific impulses are around 220 s for state-of-the-art hydrazine thruster technology). In a hydrazine thruster, the propellant is passed through a catalyst bed and decomposed. The decomposition products are nitrogen, hydrogen, and ammonia. The catalyst pellets are contained within a mesh construction in a so-called catalyst bed.

Upon contact with the iridium surfaces, the hydrazine decomposition reaction is initiated. Performances are shown in Table 1

	T [mN]	Isp [s]	mass [kg]	dimension [Ø mm]	m/T [kg/mN]
Primex MR 103	1	210	0,33	14,8x3,4	0,36667
Marquardt KMH S 10	1	226	0,33	14,6x3,2	0,36667
Daimler Chrysler	1	223	0,28		0,28
Primex MR-11E	2	213	0,33	16,9x3,8	0,15
Primex MR-111C	4	226	0,33	16,6x3,8	0,07416
Marquardt KMH S 17	4	230	0,38	20,3x3,2	0,08539
TRW MRE-1	5	220	0,82		0,164
TRW MRE-4	18	230	0,41		0,02278

Table 1 : Performance of monopropellant hydrazine thruster

### Cold gas thruster

Cold gas thruster represent the smallest rocket engine technology available today. Cold gas systems are valued for their low system complexity, their small impulse bit, and the fact that, when using benign propellant (e.g. N<sub>2</sub>) they present no spacecraft contamination problems. Cold gas systems are characterized by a low specific impulse, unless very light gases (H<sub>2</sub>, He) are used. Neither hydrogen nor helium is commonly used, however, since storage problem due to large and heavy tankage would result as a consequence of low gas density. Performance are shown in Table 2.

	T [mN]	Isp [s]	Mass [kg]	m/T [kg/mN]
Moog A	5	65	0,0073	0,00163
Moog B	5	73	0,0055	0,00104
Moog C	289		0,0130	4,5E-05
marotta	500	73	0,0500	0,0001

Table 2: Performance of cold gas thruster

### Arcjets

Low power arcjets perform well at 0.5 to 0.75 kW. Below 0.5 kW, the performance decreases, current technology does not allow for operations at microspacecraft power levels..

### Ion Thruster

The smallest ion thrusters available are the 10 cm diameter British DERA T5 and the DASA RITA thruster. A 13 cm diameter Hughes XIPS thruster with an Isp of 2585 s, overall efficiency of 51.3%, and power of 300 Watt was launched on the ASTRA 1G satellite on December 3rd, 1997. An experimental ion thruster was launched on-board the Japanese ETS-VI, but the spacecraft failed to reach its intended orbit and the test program was severely shortened. Ion thruster loss mechanisms, such as recombination, are dominated by wall effects. Reducing the physical size will therefore reduce the efficiency and Isp. Ion thrusters could be considered for microspacecraft propulsion if issues regarding these wall losses, plume neutralization, and high voltage arcing can be resolved. Performances are shown in Table 3

	T [mN]	P/T [W/mN]	Isp [s]	mass [kg]	m/T [kg/mN]	d/T [mm/mN]	efficiency
DERA T5	25	25	3110	1,7	0,068	4	0,6
DERA T8	150	26	3470	6,2	0,04133		0,65
RIT 10	10	44	3260	1	0,1		0,36
RIT 10 EVO	35	30	3700				0,67
RIT 25	25	32	3060	1,75	0,07		0,48
RIT 15PL	50	27	3600				0,67
RIT XT – Low Beam Voltage	100	24	3340				0,68
RIT XT – High Isp mode	150	33	5555				0,83
Laben Proel RMT	12	40	3600	1,6	0,13333	12,5	0,44
Hughes	18	25	2585	5	0,2809	7,30337	0,51
Hughes DS1 NSTAR	92	25	3280				0,64
JPL	31	29	3900	2,5	0,08065	4,83871	0,66
NASA Lewis	11	28	2650			7,33945	0,47
Keldysh Res center	6	27	3650			8,92857	0,66
Keldysh Res center	19	26	3500			5,26316	0,65

Table 3: Performance of ion thruster

### Hall Thruster

The SPT-100 typically provides 80 mN thrust at an Isp of 1600 s and 48% efficiency with an input power of 1.35 kW. A SPT-50 has been laboratory tested down to 0.09 kW with an Isp of 700 s and efficiency of 21% . At the design point of 0.3 kW, the SPT-50 operated at an Isp of 1160 s and an efficiency of 32%. Hall thruster scalability is critical. Performances are shown in

	T [mN]	P/T [W/mN]	Isp [s]	mass [kg]	m/T [kg/mN]	d/T [mm/mN]	efficiency
Fakel SPT-100	90	16	1712	3,5	0,0388	1,1111	0,54
SPT-70	40	16	1510			1,75	0,46
Fakel SPT-60	30	17	1300			2	0,38
Fakel SPT-50	20	18	1250	0,9	0,045	2,5	0,35
Moskow SPT-30	13	20	1234	0,4	0,0307	2,3076	0,3
Fakel SPT-25	6,4	24	948			3,9062	0,19
T-27	9,6	21	1430				0,33
T-100	82,4	16	1573			1,2135	0,47
Keldysh X-40	35	15	1750			1,1428	0,56
Keldysh KM-37	18,4	16	1635				0,49
Keldysh KM-32	10,4	15	1410				0,45
SNECM A PPS 1350	85	18	1650	4,5	0,0529	1,1764	0,46
Busek BHT -HD-600	36	17	1700	2,2	0,0611	2,7777	0,5
Busek BHT -HD-1000	55,5	18	2051	3,5	0,0630	2,5225	0,56
Busek BHT -200-X2B	17	18	1600	0,9	0,0529	5,8823	0,45
Princeton	54,4	16	1550			1,6544	0,46
Un. of Hifa	39	17	1656			1,8461	0,49
D-38	11,4	19	1336				0,34
D-35	82	15	1263	4,35	0,0530	0,6707	0,4
Keldysh K-15	16	25	1718			0,9375	0,36

Table 4: Performance of hall thruster

### Colloid Thruster

Busek Corporation is developing a colloidal thruster system in the 25 microNewton class for the SBIR Air Force early warning satellite system. Stanford University is also involved in testing small colloid thrusters. Performance are shown in Table 5

	T [mN]	P[W]	P/T [W/mN]	Isp [s]	mass [kg]	m/T [kg/mN]	efficiency
Electro optical system	0,008	0,03	4,4	700	7,33	964,47	0,78
TRW	0,001	0,01	10,3	1450			0,69
TRW/Edwards AFB	0,159	1,4	8,8	1382			0,77
TRW/Edwards AFB	0,129	1,15	8,9	1405			0,77
TRW/Edwards AFB	0,335	2,41	7,2	1029	4,95	14,798	0,7
Busek	0,189	6		400			
Stanford	0,001	0,01	10	500			0,25

Table 5: Performance of colloidal thruster

### PPT

Typical thrust levels are between 0.05 and 2 mN, Isp about 1500 s, which makes this device well suited for accurate spacecraft positioning such as the multi-spacecraft interferometric experiment. PPTs are possibly the best candidate for many micro-propulsion tasks. The minimum impulse bits obtainable are on the order of 10 mN-s, with larger impulse bits possible up to 1 mN-s. A total impulse of up to 20 kN-s is targeted for larger systems. Performance does not significantly deteriorate with power level. Total impulse and impulse bit size can be varied by changing the fuel bar geometry. Space readiness has not been reached yet. Performances are shown in Table 6

	T [mN]	P[W]	P/T [W/mN]	Isp [s]	mass [kg]	m/T [kg/mN]	efficiency
zond2	2,000			410	5	2,5	
LES 6	0,027	2,5	93	590			0,03
NOVA	0,370	30	81	850	7,1	19,189	0,05
SMS	0,160	22	138	400			0,01
LES 8/9 (MIT)	0,600	25,5	43	1000	7,33	12,216	0,12
Millipound	4,450	150	34	1210			0,18
PPT-4	0,450	15	33	1250			0,18
PPT-5	0,750	50	67	1750			0,13
OS-1	1,400	70	50	1400	4,95	3,5357	0,14
PPT	0,090	20	222		0,5	5,5555	
PPT	2,000	100	50	800			0,08
PPT	0,140	12,5	89	500			0,03
advPPT	4,200	133	32	515			0,08
APPT	5,200	250	48	1700			0,17

Table 6: Performance of PPT thruster

### FEEP

Thrust units can be quite small and have comparatively high specific impulse. Space readiness has not been proved yet. Performances are shown in Table 7

	T [mN]	P[W]	P/T [W/mN]	Isp [s]	m/T [kg/mN]	d/T [cm <sup>3</sup> /mN]	efficiency
Alta FEEP -1000	1,200	72	60	10000	4,1666		0,82
Alta FEEP -100	0,120	7,2	60	10000			0,82
ARCS inFEEP-25	0,025			10000	284		
ARCS inFEEP-100	0,100			10000			
Centrosazio	0,040	2,7	66	9000	15	9600	0,65
Centrosazio	1,400	93	66	9000	0,8571	585	

Table 7: Performance of FEEP thruster

## 2. Helicon thrusters

An helicon plasma thrusters is based on an helicon plasma [1] source specifically design to provide high plasmas-exhaust velocity. An helicon source is composed by very few physical elements:

- a feeding system able to provide the required neutral gas flow
- a glass tube where the plasma is generated
- an antenna having helix shape wrapped around the glass tube
- a system of coils placed coaxial with the glass tube to a magnetic field able to confine the plasma and to increase power deposition of the antenna

In this project the helicon source is used as the main element of the thruster. The thrust is obtained exhausting the plasma into vacuum driving it through a suitable magnetic field whose gradient is optimized to increase plasma velocity.

The thruster will implement one among the most advanced acceleration concept recently discovered: The potential drop which, under some circumstances, build-up on the exhaust zone. This phenomenon has been recently discovered at ANU (Australian National University) [2-3] and called Double Layer. A numerical study conducted at CISAS under ESA contract has shown that this mechanism can provide reacceleration up to two times the ion Bohm velocity [4].

## 3. Helicon thruster numerical models

The modeling approach here after proposed is based on three different numerical models: a) a global numerical model of the plasma source, b) a 1-D PIC code of the entire system, c) a 2-D PIC code of the entire system. The global model is used to simulate the plasma source behavior, it provides the source ionization rate, plasma density and electron temperature to the other two codes. A 1-D code named PPDL was developed specifically for this purpose. It is a hybrid code with Boltzmann electrons and drift-kinetic ions, inclusion of dominant 2D effects and high computational efficiency through implicit nonlinear Boltzmann solver. The 2-D code used was XOOPIC, freely available from University of California at Berkeley. With XOOPIC it was necessary to perform fully electrostatic simulations with kinetic electrons, resulting in long computational times in order to analyze detachment features. A combined approach proved very useful where the 1-D code was used to rapidly screen many different experimental conditions and to identify the right boundary condition. The 2-D code was then used to refine the 1-D results.

### 3.1 Plasma source numerical model

A global model has been developed to better understand experimental observations and to lead the experiment design. This approach is similar to other global models previously developed for simulating process plasma sources [9-14]. The plasma balance equations, for particles and energy, have been written for describing a uniform distributed plasma inside of a region determined by the magnetic field configuration.

Many studies have been done about interactions between plasma and neutrals, including the effect of neutral losses to ionization neutral heating [15-21]. Several models take into account the neutrals density inserting a source term and a sink term into the neutrals balance equation. These terms are related respectively with the feeding flow from the reservoir and the flow to the vacuum pump [15-20, 22-23]. In other models the plasma neutral interactions are not considered at all and no equations are written to follow the neutrals density behavior [20-21]. Due to the specific gas-dynamic configuration of the device, the neutral interaction with plasma has been considered in this work by coupling a 0-dimensional gas-dynamic model of the entire system, with a global plasma model of the source. This model provides an estimate for the pop-off feeding-valve operation, efficiency of neutral pumping by the vacuum pump, efficiency of a gas trap in the source to increase the ionization efficiency. The interactions that are taken into account in the model are:

- neutral density reduction due to ionization;
- neutral dissociation (molecular specie-atom species);
- zero dimensional gas dynamic analysis behavior in the plasma source and in the vacuum chamber;
- wall recombination and volume recombination in the main vacuum chamber.

Plasma is generated in the source chamber. A preliminary investigation shows that in specific magnetic field configurations or in a specific operation mode (helicon mode), the plasmas could be confined inside of a volume smaller than the source chamber volume. Plasma has been considered confined in a cylindrical volume  $V_c$  defined by a radius, plasma radius  $r_p$ , and having the same length than the source chamber,  $L$ . Inside this volume different species are considered for every gas. The model follows the density of all of these species. Plasmas also flows and diffuse through the external surfaces of the volume  $V_c$ . These surfaces will be named in different way to highlight the different process involved. The back axial surface is the surface in front of the feeding orifice, plasma in this zone is electrostatically confined and the mass loss is calculated using Godyac and Maximov[9]. Solution of diffusion equation. Plasma also diffuse through the radial surface, but in this zone the magnetic field generated by the solenoid coil improves the confinement. The particle loss in this area has been calculated using again the Godyac and Maximov solution modified by Cheetham [9]. To take into account the magnetic field contribute in the confinement. The axial surface toward the vacuum chamber is named exhaust surface. Plasma flows in this zone with a speed that is a fraction of the ion sound velocity. The speed strongly depend on the shape of the plasma potential in this area. Being this calculation beyond the purpose of this model, a parameter has been introduced into the numerical analysis named  $cs$ . Therefore the exhaust velocity is the ion sound velocity multiplied by the  $cs$  coefficient that has been considered as a free parameter. This coefficient is evaluated using PIC codes.

Particles that diffuse through the lateral surface and through the back axial surface are neutralized. As will be explained later, plasma equations are coupled with neutral equations since in the source chamber the neutrals density is not constant but free to change in relation to the neutral flow, the dissociation processes and the plasma-neutral interaction. The reactions involving ionized species and

electrons are found in literature. The particle balance equations for the ionized particles and electrons are written in a particle flux form, (particles/seconds m<sup>3</sup>). The general form for the balance equations of charged particles is:

$$\frac{dn_i}{dt} = G_i^s - G_i^l - G_{W_i} - G_{EXH-i} \quad (1)$$

$G_i^s$  is for the i-specie the source term due to plasma processes,  $G_i^l$  is the loss term due to plasma processes,  $G_{W_i}$  is for the i-specie the loss term due to particle recombination at the wall (the particle diffuses through the wall sheath before reaching the wall),  $G_{EXH}$  is the loss term due to the particle flow through the exhaust. The reaction rates were obtained averaging the cross section for the specific reaction over a Maxwellian distribution[10].

$$K_i = \left( \frac{m}{2pkT} \right)^{3/2} \int_0^\infty s(v) v \exp\left(-\frac{mv^2}{2kT}\right) 4\pi v^2 dv \quad (2)$$

where T is the electron temperature in eV and m is the particle mass and s the cross section. Wall losses are calculated as in[15-22]. Ions lost at the exhaust are calculated as :

$$L_{EXH} = n_i \cdot u_B \cdot A_{EXH} \cdot cs$$

$$u_B = \sqrt{\frac{kT_e}{m_i}} \quad (3)$$

$u_B$  term is the ion Bohm's velocity and  $A_{EXH}$  is the geometrical exhaust area.

Another parameter affects the exhaust flow. At the exit of the plasma discharge section magnetic field variation could build-up a magnetic mirror reflecting part of the plasma flow. Therefore the net flow is given by the difference between the incident flow and the reflected flow. The reflected flow depends on the configuration of the magnetic field and on the plasma parameters as explained later in the section "Magnetic mirror".

To calculate the electron temperature, the power balance equation has been written as follows (units: W/m<sup>3</sup>)

$$\frac{P_{ABS}}{Ve} = \frac{d}{dt} \left( \frac{3}{2} \cdot e \cdot n_e \cdot T_e \right) + \sum P_i + P_W + P_{EXH} \quad (1)$$

$P_{ABS}$  is the deposited power into the plasma that is assumed to be known. e is the electron charge,  $T_e$  is the electron temperature,  $V_e$  again the plasma volume.  $P_i$  terms are the power lost in the i-reaction. The general formula is:

$$P_i = K_i \cdot E_{TH-i} \cdot n_e \cdot n_j \quad (2)$$

where  $K_i$  is the rate constant for the specific reaction,  $E_{TH-i}$  the threshold energy for the i-reaction,  $n_e$  the electron density,  $n_j$  the density of the specie involved in the i reaction.  $P_W$  is the power lost at the wall due to the electron-ions flow.  $P_{EXH}$  is the power loss associated with the electron and the ion flux at the exhaust, assuming that the escaping velocity is the ion-Bohm velocity multiplied by cs. Experimental results [26] indicate the presence of a hot tail in the electron population in hydrogen and helium discharge. This distribution has been modeled adding two Maxwellian distributions: one with the temperature of the bulk of the plasma and one with the temperature of the hot tail. The model operates with Argon, hydrogen or helium.

The numerical outputs of the model described above were compared with experimental data found in literature [5] about plasma parameters in the helicon stage. This

operation made it possible to validate the model and to determine the value of few parameters. Figure 1 shows the comparison between the model results and experimental data found in literature.

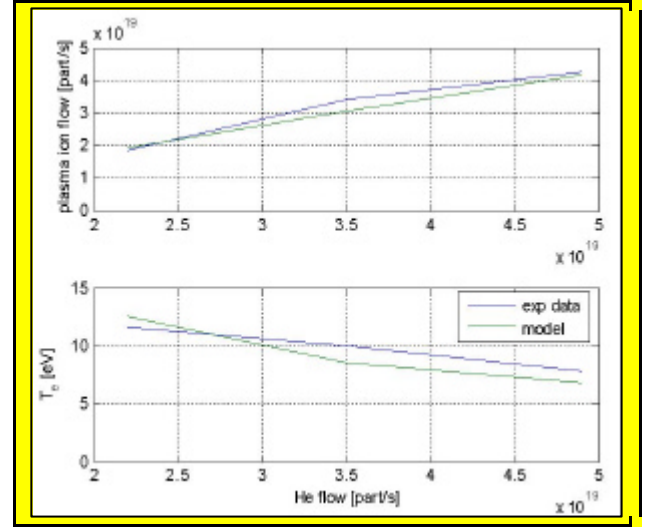


Fig. 1 Comparison between experimental data and the numerical model. Helium discharge. 3 kW RF power

### 3.2 1-d pic numerical model

PPDL[6,26] is a modified version of an existing 1-D PIC named PadPIC, a Particle in Cell [7] plasma simulator. The main features of PPDL are:

- Drift-kinetic ions, where the magnetic moment is assumed to be an adiabatic invariant. The drift kinetic equation of motion
- The expansion of the magnetic field is considered
- Boltzmann electrons, assuming Maxwellian distribution and inertialess.
- Floating boundary conditions.
- Plasma generation is simulated through a source term.

The advantage of Boltzmann electrons is that electron time scale (plasma and gyro periods) do not have to be resolved, but on the other side it requires a non-linear Poisson solver to determine the electrostatic potential. With the hybrid Boltzmann electron/drift-kinetic ion approach, the time step is only limited by ion period which is two orders of magnitude larger than electron plasma period and ion gyro period, which can become very short in a strong magnetic field, is removed. Thus, PPDL is very fast and efficient and still capable of simulating the relevant physics. To better fit the experimental set-up the presence of magnetic field is simulated by the analytic solution of a field generated by one or more solenoids. The gradient of the magnetic field is also calculated analytically and used for adding the  $\nabla B$  velocity to the drift-kinetic ions. The dilution of the charge density due to the expanding magnetic field has also been incorporated into the non linear Poisson solver.

It was considered a plasma of radius  $r_0$ , density  $n_0$ , and temperature  $T_e$  created in a uniform field  $B_0$  and then injected into a region of expanding field lines. For plasma frozen to the field lines. The expansion of  $B(z)$  and  $n(z)$  plasmas along the magnetic field is also simulated using the relation:

$$\frac{n}{n_0} = \frac{B}{B_0} = \left( \frac{r_0(z)}{r(z)} \right)^2 \quad (6)$$

where  $r(z)$  is the radius of magnetic lines at position  $z$ .

PPDL can simulate the potential drop due to source and magnetic field configuration to accelerate the plasma after its creation.

PPDL is a monodimensional code developed to simulate the potential drop acceleration of ions in the Helicon double layer thruster concepts, and it has been adapted to the simulation of this low power thruster considering both plasma source and acceleration

It performs a very fast simulation (due to maxwell electrons) of the entire system. In this way it is more suitable for the application inside a genetic algorithm to perform a design optimization.

### 3.3 2-d pic simulations

The used code is XOOPIC which is an open-source code developed by Berkeley (University of California). XOOPIC (Object-Oriented Particle-In-Cell) is a 2D-3V relativistic electromagnetic PIC code. The object-oriented paradigm provides an opportunity for advanced PIC modelling, increased flexibility, extensibility and efficiency [8,27]. XOOPIC includes 2-dimensional orthogonal grid: cartesian (x,y) or cylindrically symmetric (r,z) and moving window, it includes electrostatic and electromagnetic fields, and relativistic particles. The boundaries can be determined at runtime and include many models of emitters, collectors, wave boundary conditions and equipotentials. Because the dependence on the azimuthal angle is not expected to be relevant for DL experiments, it can be used a 2D r-z cylindrical PIC simulation. The code can handle an arbitrary number of species, particles, and boundaries. It also includes Monte Carlo collision (MCC) algorithms for modelling collisions of charged particles with a variety of neutral background gasses.

The same geometry and magnetic field configuration of PPDL was reproduced with XOOPIC to confirm and to refine the optimization results.

### 3.4 Thruster global design

The thruster has been designed through the following strategy:

Performance models described above have been combined with a lumped structural model providing, depending on the selected thruster configuration (i.e mass flow, magnetic field, power etc.), the total volume and mass

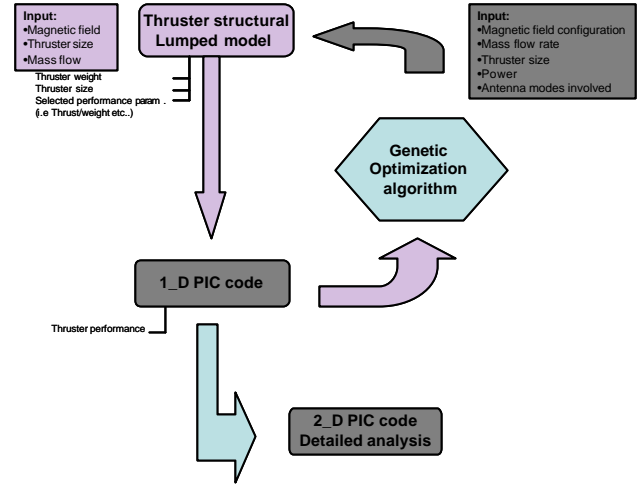


Fig. 2. Optimization logic

To perform the optimization it has been used a genetic algorithm.

The structure of the multi-objective evolutionary algorithm used in this work follows the main steps of a  $\mu + \mu$  evolution strategy. The evaluation step includes estimating the fitness functions from the actual decision variables and ranking the individuals according to the Pareto concepts. Then the Genetic Diversity Evaluation Method (GeDEM) is applied to establish a criterion for fitness assignment and to build the next population of parents. In short, the GeDEM preserves the genetic diversity of the best-so-far population of candidate solutions to the optimization problem by performing an additional evaluation after the common measure of objective fitness. This evaluation ranks the solutions according to their fitness value and their reciprocal distance as a way to give more reproduction chances to both highly-fit and highly-distant individuals. The loop starts again until the predetermined number of generations has been reached.

This algorithm has been used in order to identify the best thruster configuration as a trade off among performances, weight, and volume. The only thruster requirements has been the power available 50 W. The thruster constraints are: total mass lower than 1.6 kg, and total volume lower than 1 dm<sup>3</sup>.

The global model was initially used in combination with the structural model to identify ten most promising configurations, than all of them has been analyzed with the 1-D PIC model in order to identify three best configuration which has been finally investigated with the 2-D PIC code in order to evaluate thrust and Specific impulse.

The gas used in simulations is Argon. The reason is that it is much easier to be stored respect to helium and hydrogen and provides a reasonably high specific impulse.

The optimization variables are:

- source diameter
- mass flow rate
- Magnetic field configuration

The ratio between source diameter and length as been kept equal to 6.8 as average value retrieved in literature. For each configuration the minimum value of the magnetic field was assigned in order to allow a gyro radius equal to 1/3 of the source radius.

- The system presents a thrust lower than Hall thruster systems (SPT-70 - 40 mN, SNECMA PPS 1350 - 85 mN), but it uses less power and the mass and dimensions are significantly reduced compared to Hall Thruster (their chamber diameter is around 50-100 mm or more), moreover hall thruster works greatly at higher power.



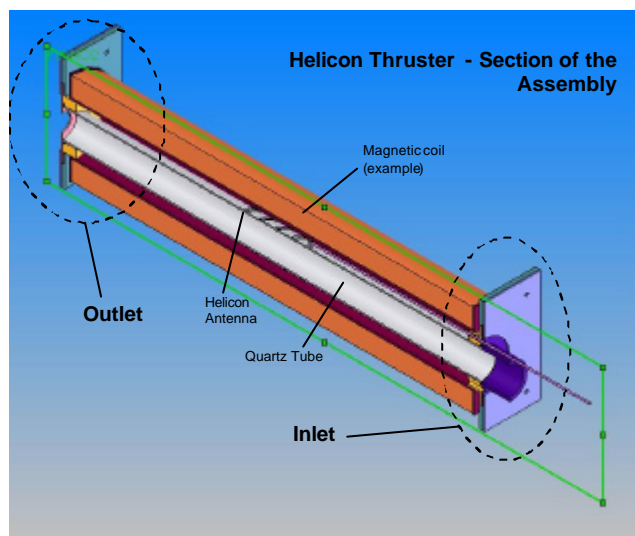
- The FEEPs have a specific impulse higher (10000s) than HPH.com system, but the thrust is limited to 0.1-0.01 mN
- PPTs (PPT-4, EOS-1) presents similar characteristic (with a smaller thrust) but the mass is higher (up to 9 kg)

As a result, the following conclusions were drawn:

- The helicon based plasma thruster propulsion system in plasma configuration presents advantages respects other propulsion system
- The system presents a compact volume and a light mass.
- The required electric power is very low (about 50 W)

### 3.4 Ongoing experimental activities

Based on the numerical results CISAS has designed an experiment to verify code results.



Georgia Institute of Technology (GA Tech) is conducting an extensive experimental characterization to verify effective thruster performances. GA Tech has the ability to operate the thruster over a forward RF power range of 50 W – 1.5 kW. Several different helicon antennas, and magnetic field configuration will be tested. All experiments are performed in GA Tech Vacuum Test Facility at an operating pressure less than  $5 \times 10^{-5}$  Torr. The thrust of the helicon thruster will be measured with a null-type inverted pendulum thrust stand. The ion exit velocity will be measured with a retarding potential analyzer.

Moreover CISAS is also conducting experimental tests in its own facility. Test results will be compared with results obtained at GA.

### 3.5 Conclusions

A mini helicon plasma thruster, has been designed at CISAS, to be mounted onboard mini satellite for attitude and position control. The thruster has been designed to operate with 50 W of power. Thruster expected performances are 1mN of thrust and 1350 s of ISP. Moreover the thruster is expected to weight 1.5 kg and to have a volume of about 1dm<sup>3</sup>.

Experimental analysis are currently ongoing in parallel at Georgia Tech University and at CISAS.

### Acknowledgment

The authors wish to thank Dr. Cinzia Giacomuzzo for her valuable work on the development of PPDL. This research has been partially supported by ESA-ARIADNA program.

### Bibliography

- 1 - C. Charles, R.W. Boswell, P. Alexander, C. Costa, O. Sutherland, L. Pfitzner, R. Franzen, J. Kingwell, A. Parfitt, P.E. Frigot, J. Gonzalez del Amo, E. Gengembre, G. Saccoccia, R. Walker, "Helicon Double Layer Thrusters" 42<sup>nd</sup> AIAA/ASME/SAE/ASEE Joint Propulsion Conference & Exhibit 9 - 12 July 2006, Sacramento, California AIAA 2006-4844
- 2 - C. Charles, "Hydrogen ion beam generated by a current-free double-layer in a helicon plasma". Applied Physics Letters 84, 332-334 (2004)
- 3 - C. Charles and R.W. Boswell, "Current-free double-layer formation in a high-density helicon discharge". Applied Physics Letters 82, 1356-1358 (2003).
- 4 - D. Pavarin, J. Carlsson, M. Manente, I. Musso, F. Angrilli, Numerical simulation of the Helicon Double Layer Thruster Concept ESA Contract No. Ariadna 05/3201
- 5 - J.P. Squire et al. "Experimental research progress toward the VASIMR engine", International electric propulsion conference 2003, Toulouse, 2003
- 6 - M. Manente, J. Carlsson, I. Musso, C. Bramanti, D. Pavarin, F. Angrilli, "Numerical simulation of the Helicon Double Layer Thruster Concept", 43rd AIAA/ASME/SAE/ASEE Joint Propulsion Conference & Exhibit, Cincinnati, OH 8-11 July 2007 - Paper AIAA 2007-5312
- 7 - C. Birdsall, A. Langdon "Plasma Physics via computer simulation" Iop, Bristol, 1991
- 8 - J.P. Verboncoeur, A.B. Langdon and N.T. Gladd, "An Object -Oriented Electromagnetic PIC Code", Comp. Phys. Comm., 87, May11, 1995, pp. 199-211
- 9- Cheetham AD, "Characterization and modelling of a helicon plasma source" J. Vac. Sci. Tech. A 16(5) Sep-Oct 1998.
- 10- Lieberman MA, "Global Model of pulse-power-modulate high-density, low-pressure discharges" Plasma Sources Sci. Tech. 5, (1996) 145-158.
- 11- C. Lee "Global Model of Plasma Chemistry in a High Density Oxygen Discharge" J.Electrochem.Soc, Vol.141, No. 6, June 1994.
- 12- S. Ashida "Spatially averaged (Global) model of time Modulated High Density Chlorine Plasmas, J.Appl.Phys. Vol. 36, (1997), pp. 854-861.
- 13- S. Ashida "Spatially averaged (global) model of time modulated high density argon plasmas", J.Vac.Sci.Tech. A 13(5), Sep/Oct 1995.
- 14- M. Meyyappan "A spatially-averaged model for high density discharges", Vacuum, Vol 47, N.3, 215-220, 1996.
- 15- M. Mozetic "Atomic hydrogen density along continuously pumped glass tube", Vacuum, vol.5, n°3-4 pp. 319-322, 1998.
- 16- G. R. Tynan "Neutral depletion and transport mechanism in large-area high density plasma sources", Journal of applied physics vol 86, n°10, Nov 1999.



- 17- C. Lee "Global model of Ar, O<sub>2</sub>, Cl<sub>2</sub>, and Ar/O<sub>2</sub> high-high density plasma discharges", J.Vac.Sci.Tech. A 13(2) Mar/Apr 1995.
- 18- T. Nakano "Ion and neutral temperature in electron cyclotron resonance plasma reactors", Appl.Phys.Lett 58(5) 1991, pp. 458-460.
- 19- J. Hopwood "Neutral gas temperature in a multipolar electron cyclotron resonance plasmas", Appl. Phys. lett 58 (22), 3 Jun,1991.
- 20- M. Meyyappan "A spatially-averaged model for high density discharges", Vacuum, Vol 47, N.3, 215-220, 1996.
- 21- B. Gordies, "Self-consistent kinetic model of low-pressure N<sub>2</sub>-H<sub>2</sub> flowing discharges II", Plasma sources Sci. Tech 7(1998), 378-388.
- 22- Suwon C, "A self consistent global model of neutral gas depletion in pulsed helicon plasmas", Physics of plasmas, vol 6, Jan 1996, pp. 359-365.
- 23- Gilland J, "Neutral Pumping in a Helicon Discharge", Plasma Sources Sci Tec n 7, 1998, pp 416-422.
- 24- Godyak V A 1986 S.
- 25- M. I. Panevsky "Characterization of the Resonant Electromagnetic Mode in Helicon Discharges" PhD Thesis, University of Texas at Austin, 2003.
- 26- Manente M., Musso I., Carlsson J., Giacomuzzo C., Bramanti C., Pavarin D. "1D-simulation of helicon double layer thruster" 30TH International Electric Propulsion Meeting Florence, Italy - September 17-20, 2007
- 27- Musso I., Manente M., Carlsson J., Giacomuzzo C., , Bramanti C., Pavarin D. "2D-OOPIC SIMULATIONS OF THE HELICON DOUBLE LAYER" 30TH International Electric Propulsion Meeting Florence, Italy - September 17-20, 2007